THE JOURNAL OF PHYSICAL CHEMISTRY B

Article

pubs.acs.org/JPCB

Formation of Nanophases in Epoxy Thermosets Containing Amphiphilic Block Copolymers with Linear and Star-like Topologies

Lei Wang, Chongyin Zhang, Houluo Cong, Lei Li, and Sixun Zheng*

Department of Polymer Science and Engineering and the State Key Laboratory of Metal Matrix Composites, Shanghai Jiao Tong University, Shanghai 200240, China

Xiuhong Li and Jie Wang

Shanghai Synchrotron Radiation Facility, Shanghai Institute of Applied Physics, Chinese Academy of Science, Shanghai 201204, P. R. China

ABSTRACT: In this work, we investigated the effect of topological structures of block copolymers on the formation of the nanophase in epoxy thermosets containing amphiphilic block copolymers. Two block copolymers composed of poly(ε-caprolactone) (PCL) and poly(2,2,2-trifluoroethyl acrylate) (PTFEA) blocks were synthesized to possess linear and star-shaped topologies. The star-shaped block copolymer composed a polyhedral oligomeric silsesquioxane (POSS) core and eight poly(ε-caprolactone)-*block*-poly(2,2,2-trifluoroethyl acrylate) (PCL-*b*-PTFEA) diblock copolymer arms. Both block copolymers were synthesized via the combination of ring-opening polymerization and reversible addition−fragmentation chain transfer/macromolecular design via the interchange of xanthate (RAFT/MADIX) process; they were controlled to have identical compositions of copolymerization and lengths of blocks. Upon incorporating both block copolymers into epoxy thermosets, the spherical PTFEA nanophases were formed in all the cases. However, the sizes of PTFEA nanophases from the star-like block copolymer were significantly lower than those from the linear diblock copolymer. The difference in the nanostructures gave rise to the different glass transition behavior of the nanostructured thermosets. The dependence of PTFEA nanophases on the topologies of block copolymers is interpreted in terms of the conformation of the miscible subchain (viz. PCL) at the surface of PTFEA microdomains and the restriction of POSS cages on the demixing of the thermoset-philic block (viz. PCL).

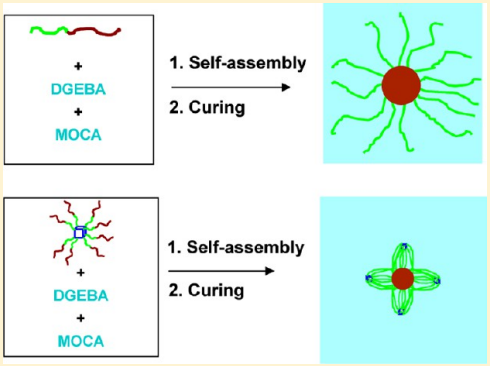

INTRODUCTION

Over the past decades, considerable progress has been made to understand the correlation of the morphological structures with the resulting properties of multicomponent thermosets.[1,2] Recently, it has been recognized that the formation of nanostructures in the multicomponent thermosets can further optimize the intercomponent interactions and thus the mechanical properties of the materials were significantly improved.[3,4] In 1997, Hillmyer et al.[5,6] first reported the formation of nanophases in thermosets with amphiphilic block copolymers via self-assembly approach. In this protocol, the precursors of thermosets act as the selective solvents of amphiphilic block copolymers and some self-organized nanophases in the mixture are created before curing reaction. These preformed nanophases can be fixed with the subsequent curing reaction and thus nanostructured thermosets can be obtained. More recently, it was realized that ordered or disordered nanostructures in thermosets can be alternatively formed via so-called reaction-induced microphase separation (RIMPS) mechanism.[7,8] In this approach, a part of subchains of the block copolymers are demixed out of the initial homogeneous mixtures with curing reaction proceeding whereas the other subchains still remain miscible with the matrix of the thermosets.

The importance of the nanophase formation in thermosets is profound for either the improvement in mechanical properties of thermosets or the development of other nanostructured materials with new and functional properties. It is found that toughening of thermosets via the formation of nanostructures is quite dependent on morphology of nanophases in thermosets. The mechanisms of toughness improvement could involve either the debonding of micelles (or vesicles) from thermosetting matrix or crack deflection and frictional interlocking for the thermosets possessing the terraced morphology.[9−12] In addition to significant improvement in fracture toughness, it is realized that the nanostructured thermosets could be a class of versatile precursors to other nanomaterials with new and functional properties.[13−17] For instance, the

Received: February 28, 2013
Revised: June 7, 2013
Published: June 14, 2013

dx.doi.org/10.1021/jp402084u | *J. Phys. Chem. B* 2013, 117, 8256−8268

nanostructured phenolic thermosets containing amphiphilic block copolymers have been used as the precursors to obtain mesoporous carbon materials via pyrolysis at elevated temperatures.[18] More recently, Hillmyer et al.[19] reported the preparation of nanoporous poly(norbornenylethylstyrene-*s*-styrene) by the use of the nanostructured thermosets from dicyclopentadiene and poly(norbornenylethylstyrene-*s*-styrene)-*block*-polylactide diblock copolymer via the removal of polylactide nanophases from the thermosets.

It is critical to investigate the formation of nanophases in thermosets to establish the relation between nanostructures and physical properties of the materials. Since Hillmyer et al.[5,6] first reported the formation of ordered spherical nanophases in epoxy thermosets containing poly(ethylene oxide)-*block*-poly(ethylethylene) diblock copolymer, other ordered or disordered nanophases with a broad variety of morphologies have been reported to form in the thermosets by the use of different block copolymers via self-assembly or RIMPS approach.[18−51] It is proposed that nonlinear architecture of block copolymers could exert additional variables to influence the formation of nanophases in thermosets and thus the nanostructures of thermosets can be modulate by the topologies of these copolymers. For instance, Serrano et al.[34,41,49] first reported the formation of ordered nanostructures in epoxy thermosets containing epoxidized star-shaped polystyrene-*block*-polybutadiene block copolymer. Meng et al.[43] investigated the formation of nanophases in epoxy thermosets containing the binary block copolymers composed of PCL and PS with linear and star-like topologies. The RIMPS of the tetra-armed star-like block copolymer yielded the lamellar nanophases in the thermosets, which is in marked contrast to the formation of spherical nanophases in the thermosets containing the linear diblock copolymer. More recently, Zhu et al.[52] reported the formation of nanophases in epoxy thermosets containing an organic−inorganic macrocyclic molecular brush with poly(ε-caprolactone)-*block*-polystyrene side chains. However, such investigations remain largely unexplored vis-à-vis the studies on the formation of nanophase in thermosets by the use of the block copolymers with linear architectures.

In this work, we reported the investigations on the formation of nanophases in epoxy thermosets containing poly(ε-caprolactone)-*block*-poly(2,2,2-trifluoroethyl acrylate) block copolymers with linear and star-like topologies. The star-like block copolymer is composed of a polyhedral oligomeric silsesquioxane (POSS) core and eight poly(ε-caprolactone)-*block*-poly(2,2,2-trifluoroethyl acrylate) (PCL-*b*-PTFEA) diblock copolymer arms. Both block copolymers were synthesized via the combination of ring-opening polymerization (ROP) and reversible addition−fragmentation chain transfer/macromolecular design via the interchange of xanthate (RAFT/MADIX) process with identical compositions of copolymerization and the lengths of blocks. The formation of nanophases in epoxy thermoset containing these two block copolymers were investigated by means of atomic force microscopy (AFM), small-angle X-ray scattering (SAXS) and dynamic mechanic thermal analysis (DMTA).

EXPERIMENTAL SECTION

Materials. Diglycidyl ether of Bisphenol A (DGEBA) with the epoxide equivalent weight of 185−210 was purchased from Shanghai Resin Co. 2,2,2-Trifluoroethyl acrylate (TFEA) was of chemically pure grade, obtained from Shanghai Reagent Co. ε-Caprolactone (CL) (99%) was purchased from Fluka Co. Before use, the inhibitor in TFEA was removed by passing through a neutral alumina column. Both CL and TFEA were distilled over calcium hydride (CaH_2) under reduced pressure. Stannous octanoate [$Sn(Oct)_2$] was purchased from Aldrich Co. Octavinyl polyhedral oligomeric silsesquioxane (POSS) was purchased from Amwest Technology Co., Shenyang, China. Other reagents such as β-mercaptoethanol, 4,4′-methylenebis(2-chloroaniline) (MOCA), benzyl alcohol, 2-bromopropyl bromide, and copper(I) bromide were of analytically pure grade, supplied by Shanghai Reagent Co.. The solvents such as toluene and tetrahydrofuran (THF) were dried by refluxing over sodium and subsequent distillation. 2,2-Azobisisobutylnitrile (AIBN) was of chemically pure grade, supplied by Shanghai Reagent Co.; it was purified by recrystallization from ethanol and dried in vacuo at room temperature. All the other reagents were purified according to the standard procedures.

Synthesis of Octa(2-hydroxyethylthioethyl) POSS. To a flask equipped with a magnetic stirrer were charged octavinyl POSS (4.000 g, 6.32 mmol), β-mercaptoethanol (4.344 g, 52.6 mmol), AIBN (0.422 g, 2.78 mmol) and toluene (160 mL). The solution was purged with highly pure nitrogen for 30 min to eliminate oxygen. The mixtures were heated to 70 °C with vigorous stirring and maintained at this temperature for 24 h. After that, toluene and excess β-mercaptoethanol were removed via rotary evaporation. The crude products were dissolved in tetrahydrofuran and precipitated with diethyl ether. This procedure was repeated three times to purify the sample. The product (2.26 g) was obtained with the yield of 71.1%. ^{1}H NMR (acetone-d_6, ppm): 3.96 (t, 1H, $HO-CH_2-CH_2-S$), 3.68 (m, 2H, $HO-CH_2-CH_2-S$), 2.72 (m, 2H, $HO-CH_2-CH_2-S$), 2.67 (t, 2H, $S-CH_2-CH_2-Si$), 1.07(t, 2H, $S-CH_2-CH_2-Si$).

Synthesis of POSS[PCL-OH]$_8$. To a flask equipped with a magnetic stirrer were charged octa(2-hydroxyethylthioethyl) POSS (0.1850 g, 0.147 mmol with respect of hydroxyl groups) and anhydrous toluene (15.0 mL), and the system was dried via azotropic distillation. Cooled to room temperature, CL (6.50 g, 57 mmol) and $Sn(Oct)_2$ dissolved in anhydrous toluene (0.2 wt % with respect of ε-caprolactone) were added. The system was degassed via three pump−thaw−freeze cycles and then immersed in a thermostated oil bath at 120 °C for 24 h. The polymerized product was dissolved with THF and then precipitated with a great amount of petroleum ether (distillation 60−90 °C). This procedure was repeated three times to purify the sample. The precipitates were filtered and dried in vacuo at 30 °C for 24 h to afford the polymer (6.48 g) with the yield of 97%. ^{1}H NMR ($CDCl_3$, ppm): 4.19 (t, 2H, $SiCH_2CH_2SCH_2CH_2$), 4.04 (t, 92H, $COOCH_2CH_2CH_2CH_2$), 3.63 (t, 2H, $HOCH_2CH_2CH_2$), 2.73 (t, 2H, $SiCH_2CH_2SCH_2-$), 2.63 (t, 2H, $Si-CH_2-CH_2-S$), 2.29 (t, 92H, $OCOCH_2CH_2CH_2$), 1.64 (m, 184H, $OCOCH_2CH_2CH_2CH_2$), 1.37 (m, 92H, $OCOCH_2CH_2CH_2CH_2$), 1.02 (t, 2H, SCH_2CH_2Si). GPC: M_n = 36 600 with M_w/M_n = 1.29.

Synthesis of POSS[PCL-OOCCHCH$_3$-SSCOC$_2$H$_5$]$_8$. First, to a flask equipped with a dried magnetic stirrer were charged the above PCL star with POSS core (6.20 g, 1.35 mmol with respect of hydroxyl groups) and 50 mL anhydrous toluene, and the system was dried via azotropic distillation. Cooled to room temperature, THF (60 mL), triethylamine (0.17 mL), and 2-bromoisobutyl bromide (4.0 g, 18.53 mmol) were charged; the reaction was performed at 0 °C for 1 h and at room temperature for 24 h. After the solids were removed via

dx.doi.org/10.1021/jp402084u | J. Phys. Chem. B 2013, 117, 8256−8268

filtration, the solution was concentrated via rotary evaporation and dropped into a great amount of cold methanol to afford the precipitates. The precipitates were redissolved in THF and the as-obtained solution was dropped into 200 mL of methanol to afford the precipitates. After drying in a vacuum oven at 30 °C for 24 h, the product (4.07 g) [denoted POSS[PCL-OOCCBr$(CH_3)_2]_8$] was obtained with the yield of 75.1% ^{1}H NMR ($CDCl_3$, ppm): 4.35 (m, 1H,OCOC*H*BrCH$_3$), 4.19 (t, 2H, SiCH$_2$CH$_2$SCH$_2$C*H*$_2$), 4.05 (t, 92H, COOC*H*$_2$-CH$_2$CH$_2$CH$_2$), 2.74 (t, 2H, SiCH$_2$CH$_2$SC*H*$_2$−), 2.64 (t, 2H, SiCH$_2$C*H*$_2$−S), 2.30 (*t*, 92H, OCOC*H*$_2$CH$_2$CH$_2$), 1.80 (d, 3H, OCOCHBrC*H*$_3$), 1.64 (m, 184H, OCOCH$_2$C*H*$_2$CH$_2$C*H*$_2$), 1.37 (m, 92H, OCOCH$_2$CH$_2$C*H*$_2$CH$_2$), 1.02 (t, 2H, SCH$_2$C*H*$_2$Si).

Second, to a flask equipped with a magnetic stirrer were charged the above POSS[PCL-OOCCHCH$_3$Br]$_8$ (3.50 g, 0.765 mmol with respect of 2-bromoisobutyl group), anhydrous pyridine (18 mL), and dichloromethane (25 mL). Thereafter, potassium ethyl xanthate (2.10 g, 13.1 mmol)[53] was added to the flask with vigorous stirring; this reaction was performed at room temperature for 36 h. After the insoluble solids were removed via filtration, the solution was concentrated via rotary evaporation and then dropped into 200 mL of cold methanol to afford the precipitates. The precipitates were redissolved in dichloromethane and reprecipitated into cold methanol. This procedure was repeated three times to purify the samples and the product [viz. POSS[PCL-OOCCHCH$_3$-SSCOC$_2$H$_5$]$_8$] (3.18 g) was obtained with the yield of 89%. ^{1}H NMR ($CDCl_3$, ppm): 4.63 (m, 2H, CH$_3$C*H*$_2$OCSS−), 4.35 (m, 1H, OCOC*H*SCSOCH$_2$), 4.19 (t, 2H, SiCH$_2$CH$_2$SCH$_2$C*H*$_2$), 4.05 (t, 92H, COOC*H*$_2$CH$_2$CH$_2$CH$_2$), 2.74 (t, 2H, SiCH$_2$-CH$_2$SC*H*$_2$−), 2.64 (t, 2H, SiCH$_2$C*H*$_2$S), 2.30 (t, 92H, OCOC*H*$_2$CH$_2$CH$_2$), 1.64 (m, 184H, OCOCH$_2$C*H*$_2$CH$_2$C*H*$_2$), 1.55 (d, 2H, CH$_3$C*H*$_2$OCSS−), 1.37 (m, 92H, OCOCH$_2$-CH$_2$C*H*$_2$CH$_2$), 1.02 (t, 2H, SCH$_2$C*H*$_2$Si).

Synthesis of POSS[PCL-*b*-PTFEA]$_8$. Typically, to a flask equipped with a magnetic stirrer were charged POSS[PCL-OOCCHCH$_3$-SSCOC$_2$H$_5$]$_8$ (1.00 g, 0.062 mmol), TFEA (1.50 g, 9.73 mmol), 1,4-dioxane (2 mL), and AIBN (6.3 mg, 0.039 mmol) with vigorous stirring. The flask was connected onto a Schlenk line to degas via three freeze−pump−thaw cycles. The polymerization was performed at 70 °C for 2 h to attain the desired conversion of monomer. The crude product was dissolved with THF (10 mL), and the solution was dropped into 200 mL of cold petroleum ether to afford the precipitates. After drying in a vacuum oven at 30 °C for 12 h, the polymer (i.e., POSS[PCL-*b*-PTFEA]$_8$) (1.72 g) was obtained with the conversion of the monomer to be ca. 48%. GPC: M_n = 55 900 with M_w/M_n = 1.65.

Synthesis of PCL-*b*-PTFEA Diblock Copolymer. First, monohydroxyl-terminated poly(ε-caprolactone) (PCL-OH) was synthesized via the ring-opening polymerization (ROP) of ε-CL with benzyl alcohol as the initiator and Sn(Oct)$_2$ was used as the catalyst. Typically, benzyl alcohol (0.2040 g, 1.89 mmol) and CL (10.00 g, 87.61 mmol) were charged to a 100 mL round-bottom flask equipped with a dry magnetic stirring bar and Sn(Oct)$_2$ (1/1000 wt with respect to ε-CL) was added using a syringe. The flask was connected to a Schlenk line, and the system was degassed via three pump−freeze−thaw cycles and then immersed in a thermostated oil bath at 120 °C for 24 h. The polymerized product was dissolved in THF, and the solution was dropped into 200 mL of petroleum ether to afford the procipitates. This procedure was repeated three times to obtain the polymer with the yield of 97%. The molecular weight of PCL-OH was estimated by means of ^{1}H NMR spectroscopy to be M_n = 5130.

Second, the reaction between the above monohydroxyl-terminated PCL (PCL-OH) and 2-bromopropyl bromide was carried out to afford PCL-OOCCHBr-CH$_3$,[54] which was then reacted with potassium ethyl xanthate to obtain the xanthate-terminated PCL. The latter was used as the macromolecular chain transfer agent (CTA) to synthesize PCL-*b*-PTFEA diblock copolymer through reversible addition−fragmentation chain transfer/macromolecular design with the interchange of xanthate (RAFT/MADIX) approach. Typically, to a flask equipped with a magnetic stirrer the above xanthate-terminated PCL (1.50 g, 0.292 mmol with respect of xanthate), TFEA (2.250 g, 14.6 mmol), 1,4-dioxane (2 mL), and AIBN (9.50 mg, 0.039 mmol) were charged. The flask was connected onto a Schlenk line to degas via three pump−freeze−thaw cycles and then immersed in a thermostated oil bath at 70 °C, and the polymerization was performed for 2 h. Thereafter, 10 mL of THF was added to the flask to dissolve the reacted product; the solution was dropped into 200 mL of cold petroleum ether to obtain the precipitates. This procedure was repeated three times to purify the sample. The precipitates were dried in vacuo at 30 °C for 12 h and the product (i.e., PCL-*b*-PTFEA diblock copolymer) (2.52 g) was obtained with the conversion of TFEA to be 40.5%. GPC: M_n = 9300 with M_w/M_n = 1.30.

Preparation of Nanostructured Thermosets. The desired amount of POSS[PCL-*b*-PTFEA]$_8$ (or PCL-*b*-PTFEA) was added to the preweighed DGEBA with continuous stirring, and then the curing agent (i.e., MOCA) was added with vigorous stirring until the homogeneous mixture was obtained. The mixture was poured into a Teflon mold in which the curing reaction was performed at 150 °C for 3 h plus 180 °C for 2 h.

Measurement and Characterization. *Nuclear Magnetic Resonance Spectroscopy (NMR).* The samples were dissolved in deuterated chloroform, and the NMR spectra were measured on a Varian Mercury Plus 400 MHz NMR spectrometer with tetramethylsilane (TMS) as the internal reference.

Gel Permeation Chromatography (GPC). The molecular weights and molecular weight distribution of the polymers were measured at 70 °C on a Perkin-Elmer Series 200 system (100 μL injection column, 10 μm PL gel 300 mm × 7.5 mm mixed B columns) equipped with a reflect index detector. *N*,*N*-Dimethylformamide (DMF) containing 0.01 mol/L lithium bromide was used as the eluent at a flow rate of 1.0 mL/min. The column system was calibrated by standard polystyrenes.

Transmission Electron Microscopy (TEM). Transmission electron microscopy (TEM) was performed on a JEOL JEM-2010 high-resolution transmission electron microscope at an acceleration voltage of 120 kV. The samples were trimmed using a microtome machine, and the section samples were stained with RuO_4 to increase the contrast. The stained specimen sections (ca. 70 nm in thickness) were placed in 200 mesh copper grids for observations.

Small Angle X-ray Scattering (SAXS). The SAXS measurements were carried out on a small-angle X-ray scattering station (BL16B1) with a long-slit collimation system in the Shanghai Synchrotron Radiation Facility (SSRF), Shanghai, China, in which the third generation of synchrotron radiation light sources was employed. Two-dimensional diffraction patterns were recorded using an image intensified CCD detector. The experiments were carried out with the radiation of X-ray with

dx.doi.org/10.1021/jp402084u | J. Phys. Chem. B 2013, 117, 8256−8268

Scheme 1. Synthesis of POSS[PCL-*b*-PTFEA]$_8$ Diblock Copolymer

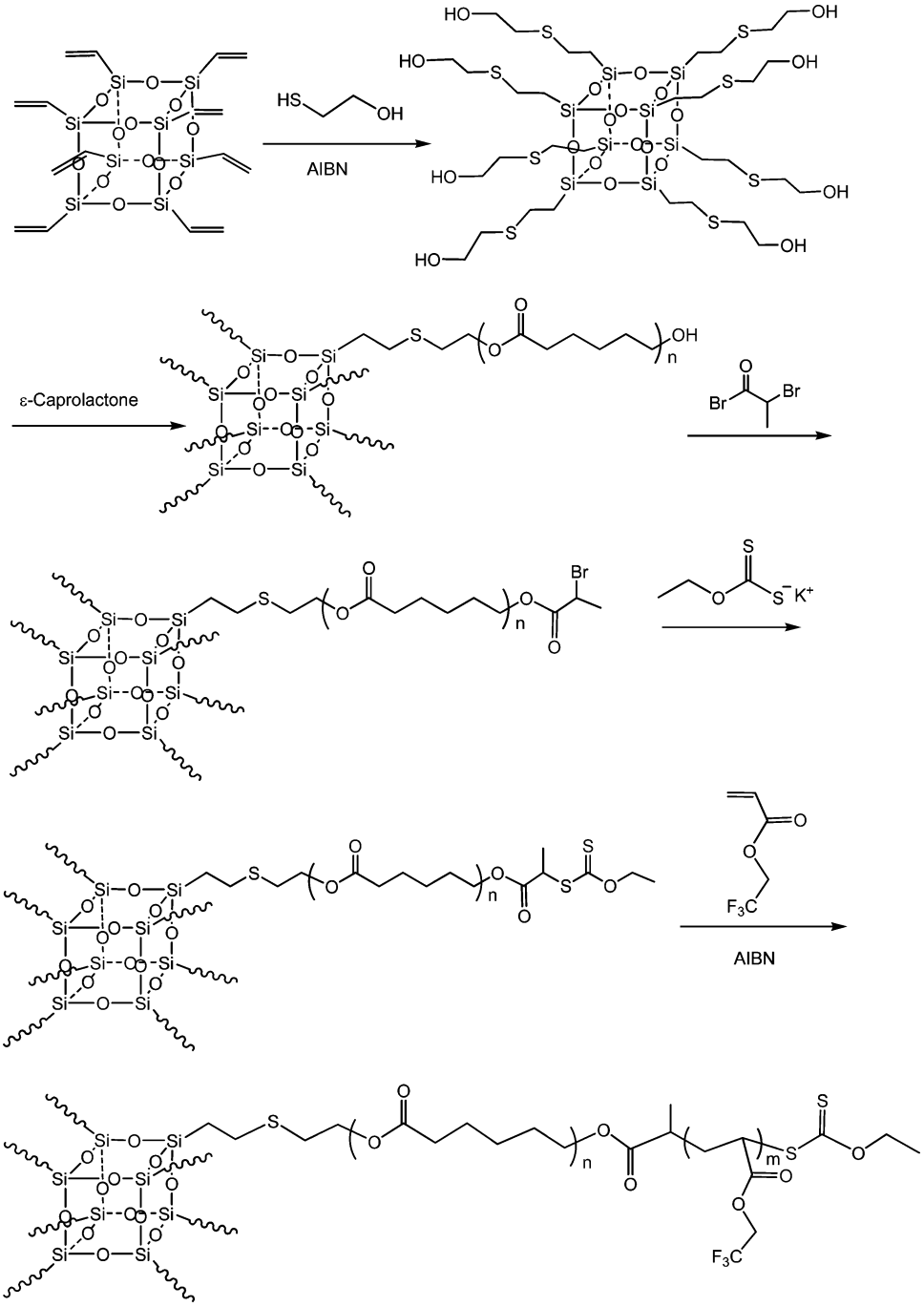

the wavelength of λ = 1.24 Å. The intensity profiles were output as the plot of scattering intensity (I) versus scattering vector, q = $(4\pi/\lambda)\sin(\theta/2)$ (θ = scattering angle).

Dynamic Mechanical Thermal Analysis (DMTA). Dynamic mechanical tests were carried out on a TA Instruments DMA Q800 dynamic mechanical thermal analyzer (DMTA) equipped with a liquid nitrogen apparatus in a single cantilever mode. The frequency used was 1.0 Hz, and the heating rate of 3.0 °C/min was used. The specimen dimension was 25 × 5.0 × 1.75 mm^3. The experiments were carried out from −80 to +220 °C.

RESULTS AND DISCUSSION

Synthesis of POSS[PCL-*b*-PTFEA]$_8$ and PCL-*b*-PTFEA. The route of synthesis for the organic−inorganic star-like block copolymer (i.e., POSS[PCL-*b*-PTFEA]$_8$) was shown in Scheme 1. First, the star-like PCL with POSS core (denoted POSS[PCL-OH]$_8$) was synthesized via the ring-opening polymerization (ROP) of ε-caprolactone (CL) with octa(2-hydroxyethylthioethyl) POSS as the initiator. The POSS[PCL-OH]$_8$ was reacted with 2-bromoisopropyl bromide to obtain POSS[PCL-OOCCHCH$_3$Br]$_8$, the terminal groups (viz. 2-bromoisopropyl) of which were further allowed to react with potassium ethyl xanthate to afford POSS[PCL-OOCCHCH$_3$-SSCOC$_2$H$_5$]$_8$, i.e., the macromolecular chain transfer agent (CTA). With the star-like macromolecular CTA, the star-like block copolymer with a POSS core and eight PCL-*b*-PTFEA diblock copolymer arms were synthesized via the reversible addition−fragmentation chain transfer/macromolecular design

dx.doi.org/10.1021/jp402084u | J. Phys. Chem. B 2013, 117, 8256−8268

with the interchange of xanthate (RAFT/MADIX) approach. In this work, octa(2-hydroxyethylthioethyl) POSS was synthesized via the thiol−ene radical addition reaction between octavinyl POSS and β-mercaptoethanol. Shown in Figure 1 are the ^{1}H NMR spectra of octavinyl POSS and octa(2-hydroxyethylthioethyl) POSS. For octavinyl POSS, the signals of resonance at 5.5−6.6 ppm are assignable to vinyl protons. The signals of resonance completely disappeared after the thiol−ene radical addition reaction. Concurrently, the new signals of resonance appeared at 1.07, 2.62, 3.69, and 3.97 ppm, and they are assignable to the protons of the methylene groups connected to silicon atom, sulfur atom, hydroxyl and terminal hydroxyl groups, respectively. The ^{1}H NMR spectroscopy indicates that all the vinyl groups of the POSS macromer were transformed into 2-hydroxyethylthioethyl groups. Shown in Figure 2 are the ^{1}H NMR spectra of POSS[PCL-OH]$_8$, POSS[PCL-OOCCHCH$_3$Br]$_8$, POSS[PCL-OOCCHCH$_3$-SSCOC$_2$H$_5$]$_8$, and POSS[PCL-*b*-PTFEA]$_8$. For POSS[PCL-OH]$_8$, the signals of proton resonance characteristic of PCL block were detected at 4.05, 3.63, 2.29, 1.63, and 1.27 ppm, respectively. In addition, the signals of proton resonance at 1.07, 2.62, and 2.74 assignable to the POSS core were discernible, indicating that the resulting product combined the structural features from POSS and PCL. The signal of resonance at 3.63 ppm is assignable to the protons of methylene groups at PCL chain ends. According to the ratio of integral intensity of methylene proton resonance at 3.63 ppm to methylene protons in the midchain of PCL, the length of each PCL arm was estimated to ca. M_n = 5140. After the esterification of POSS[PCL-OH]$_8$ with 2-bromoisopropyl bromide, the signal of resonance at 3.63 ppm completely disappeared and, in the meantime, there appeared a sharp peak at 1.82 ppm, which is assignable to the resonance of methyl protons in 2-bromopropyl groups at the chain ends of PCL. This observation suggests that all the terminal hydroxymethyl groups of PCL chains were capped with 2-bromopropyl group; i.e., POSS[PCL-OOCCHCH$_3$Br]$_8$ was successfully obtained. It is seen that with the reaction of POSS[PCL-OOCCHCH$_3$Br]$_8$ with potassium ethyl xanthate, the sharp peak at 1.82 ppm completely shifted to 1.56 ppm. Concurrently, there appeared a new signal of resonance at 4.63 ppm assignable to the protons of methylene groups in xanthate moiety. The ^{1}H NMR spectroscopy indicates that the macromolecular CTA, i.e., POSS[PCL-OOCCHCH$_3$-SSCOC$_2$H$_5$]$_8$, was successfully obtained. POSS[PCL-OOCCHCH$_3$-SSCOC$_2$H$_5$]$_8$ was used to obtain the star-like PCL-*b*-PTFEA block copolymer with POSS core (i.e., POSS-[PCL-*b*-PTFEA]$_8$) via the RAFT/MADIX approach of 2,2,2-trifluoroethyl acrylate (TFEA). In the ^{1}H NMR spectrum of POSS[PCL-*b*-PTFEA]$_8$, the signal of resonance at 4.47 ppm is assignable to methylene protons connected to the trifluoroethyl group and the signal of resonance at 2.44 ppm to the protons of the methylene in the main chain of the PTFEA block besides those signals of protons assignable to the POSS core and PCL block. The ^{1}H NMR spectroscopy indicates that the resulting polymer combined the structural features from POSS, PCL, and PTFEA chains. According to the ratio of integral intensity of proton resonance at 1.76 ppm from PTFEA block to that at 4.07 ppm from PCL block together with the length of PCL block (viz. $L_{PCL,NMR}$ = 5140 Da), the length of each PTFEA block in POSS[PCL-*b*-PTFEA]$_8$ was estimated to be $L_{PTFEA,NMR}$ = 4160 Da. Both POSS[PCL-OH]$_8$ and POSS-[PCL-*b*-PTFEA]$_8$ were subjected to gel permeation chromatography (GPC) to measure their molecular weights and the GPC curves are shown in Figure 3. For POSS[PCL-OH]$_8$ and POSS[PCL-*b*-PTFEA]$_8$, the molecular weights were measured to be M_n = 36 600 with M_w/M_n = 1.29 and M_n = 55 900 with M_w/M_n = 1.65, respectively. The unimodal distribution of

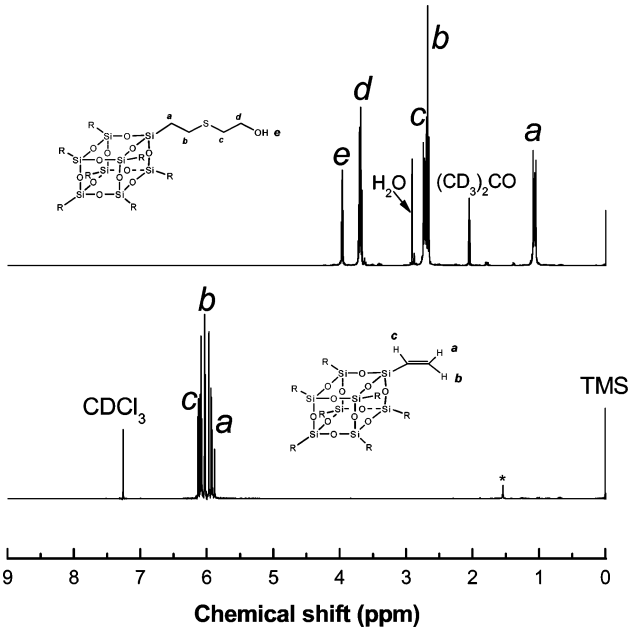

Figure 1. ^{1}H NMR spectra of octavinyl POSS and octa(2-hydroxyethylthioethyl) POSS. *: the resonance is responsible for a trace of water in the deuterium acetone.

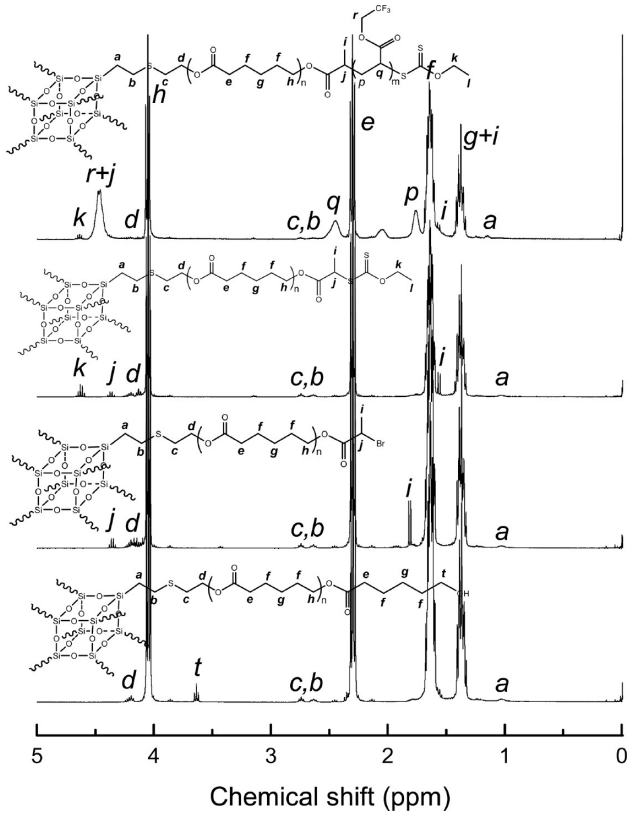

Figure 2. ^{1}H NMR spectra of POSS[PCL-OH]$_8$, POSS[PCL-OOCCHCH$_3$Br]$_8$, POSS[PCL-OOCCHCH$_3$SSCOC$_2$H$_5$]$_8$, and POSS[PCL-*b*-PTFEA]$_8$.

dx.doi.org/10.1021/jp402084u | J. Phys. Chem. B 2013, 117, 8256−8268

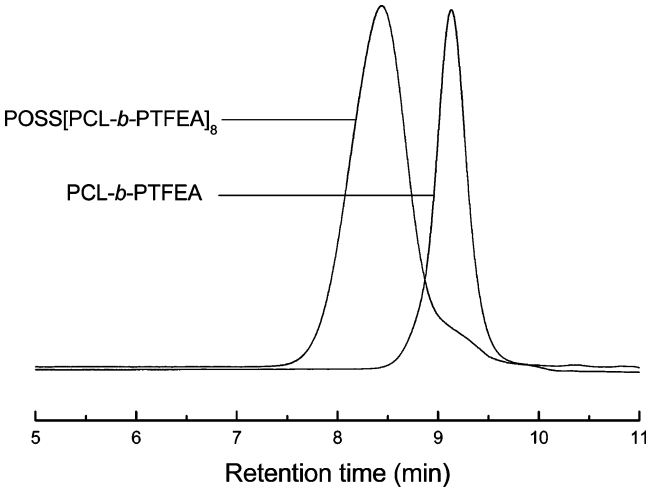

Figure 3. GPC curves of POSS[PCL-*b*-PTFEA]$_8$ and PCL-*b*-PTFEA diblock copolymers.

molecular weights as well as a narrow polydispersity of molecular weights suggests that the polymerizations (i.e., ROP and RAFT/MADIX) were carried out in a living manner. In terms of the results of GPC, the lengths of PCL and PTFEA chains in POSS[PCL-*b*-PTFEA]$_8$ were calculated to be $L_{PCL,GPC}$ = 4430 Da and $L_{PTFEA,GPC}$ = 2400 Da, respectively. It should be pointed out that the values of the block lengths according to GPC measurements were significantly lower than those with ^{1}H NMR spectroscopy (Table 1). This phenomenon could be explained as below. On the one hand, the star-like polymers could possess lower hydrodynamic volume than their linear counterparts with identical molecular weights. On the other hand, the measurements of molecular weights with GPC with styrene standard for the amphiphilic diblock copolymer could be subject to some underestimation due to the difference in solvation of both the blocks in DMF solution. It is proposed that for the star-like polymers, ^{1}H NMR spectroscopy would give the results of molecular weights more reasonable than the measurement of GPC. Therefore, we adopted the values of block lengths determined by ^{1}H NMR spectroscopy other than the results of GPC while we synthesized PCL-*b*-PTEEA diblock copolymer (denoted PCL-*b*-PTFEA) as the linear counterpart of POSS[PCL-*b*-PTFEA]$_8$. ^{1}H NMR spectroscopy showed that PCL-*b*-PTFEA possessed the molecular weight of M_n = 9400, in which the lengths of PCL and PTFEA blocks were L_{PCL} = 5230 and L_{PTFEA}= 4170, which are quite close to the values of POSS[PCL-*b*-PTFEA]$_8$ measured by ^{1}H NMR spectroscopy. It should be pointed out that the molecular weight of the linear PCL-*b*-PTFEA diblock copolymer estimated by ^{1}H NMR spectroscopy is in good agreement with the result of GPC measurement with M_n = 9300 with M_w/M_n = 1.30. According to the lengths of blocks in POSS[PCL-*b*-PTFEA]$_8$ and PCL-*b*-PTFEA diblock copolymer, the mass fractions of PCL and PTFEA blocks were obtained to be f_{PCL} = 0.55 and f_{PTFEA} = 0.45, respectively.

Nanostructures of Epoxy Thermosets. The block copolymers [i.e., POSS[PCL-*b*-PTFEA]$_8$ and/or PCL-*b*-PTFEA)] with star-like and linear topologies were incorporated into epoxy to investigate the formation of nanophases in the thermosets. Before the curing reaction, all the mixtures composed of the precursors of epoxy (i.e., DGEBA + MOCA) and the block copolymers were homogeneous and transparent, suggesting that no macroscopic phase separation occurred. The mixtures were cured at elevated temperatures and the thermosets were obtained with the contents of the block copolymers up to 40 wt %. It was observed that all the cured thermosets were still homogeneous and transparent. The morphologies of the thermosets were investigated by means of transmission electron microscopy (TEM) and small-angle X-ray scattering (SAXS). The TEM micrographs of the thermosets containing POSS[PCL-*b*-PTFEA]$_8$ and PCL-b-PTFEA are shown in Figures 4 and 5, respectively. Prior to the morphological observation, the specimens of ultrathin sections were stained with RuO_4 to increase the contrast of electron density between epoxy matrix and PTFEA microdomains. In this case, epoxy matrix was oxidized by RuO_4 whereas the PTFEA microdomains remained less affected. The results of TEM showed that in all the cases the epoxy thermosets displayed the microphase-separated structures, in which the spherical microdomains were dispersed into the continuous matrices (Figures 4 and 5). The white spherical nanophases are assignable to PTFEA blocks whereas the dark continuous matrices are attributed to the epoxy that was miscible with PCL blocks. For the thermosets containing POSS[PCL-*b*-PTFEA]$_8$, the sizes of the spherical PTFEA microdomains was about 10−20 nm in diameter. With increasing content of POSS[PCL-*b*-PTFEA]$_8$, the number of PTFEA microdomains increased whereas the sizes of the microdomains were less changed (Figure 4A−D). For the thermosets containing PCL-*b*-PTFEA, the sizes of the spherical PTFEA microdomains were quite dependent on the content of PCL-*b*-PTFEA. It is seen that the size of PTFEA microdomains significantly increased with increasing the content of PCL-*b*-PTFEA. For the thermosets containing 10 and 20 wt % of PCL-*b*-PTFEA, PTFEA microdomains 10−20 nm in diameter were dispersed into continuous epoxy matrices. For the thermosets containing 30 and 40 wt % of PCL-*b*-PTFEA, the sizes of PTFEA microdomains were increased to 30−40 nm in diameter.

The morphologies of the thermosets containing POSS[PCL-*b*-PTFEA]$_8$ and/or PCL-*b*-PTFEA were further investigated by means of small-angle X-ray scattering (SAXS). Shown in Figures 6 and 7 are the SAXS profiles of epoxy thermosets containing POSS[PCL-*b*-PTFEA]$_8$ and PCL-*b*-PTFEA, respectively. It is seen that these thermosets displayed the scattering

Table 1. Molecular Weights and Polydispersity of POSS[PCL-OH]$_8$, POSS[PCL-*b*-PTFEA]$_8$, and PCL-*b*-PTFEA Block Copolymers

samples	$L_{PCL,NMR}$ [b]	$L_{PTFEA,NMR}$	$M_{n,NMR}$	$L_{PCL,GPC}$ [a]	$L_{PTFEA,GPC}$	$M_{n,GPC}$	M_w/M_n
POSS[PCL-OH]$_8$	5100		42000	4430		36600	1.29
POSS[PCL-*b*-PTFEA]$_8$	5140	4160	75600	4430	2400	55900	1.65
PCL-*b*-PTFEA	5230	4170	9400	5100	4300	9300	1.30

[a]Molecular weights (or lengths) were measured by end group analysis with ^{1}H NMR spectroscopy; [b]Molecular weights (or lengths) were measured by means of gel permeation chromatography (GPC) with polystyrene standard and DMF solutions.

dx.doi.org/10.1021/jp402084u | J. Phys. Chem. B 2013, 117, 8256−8268

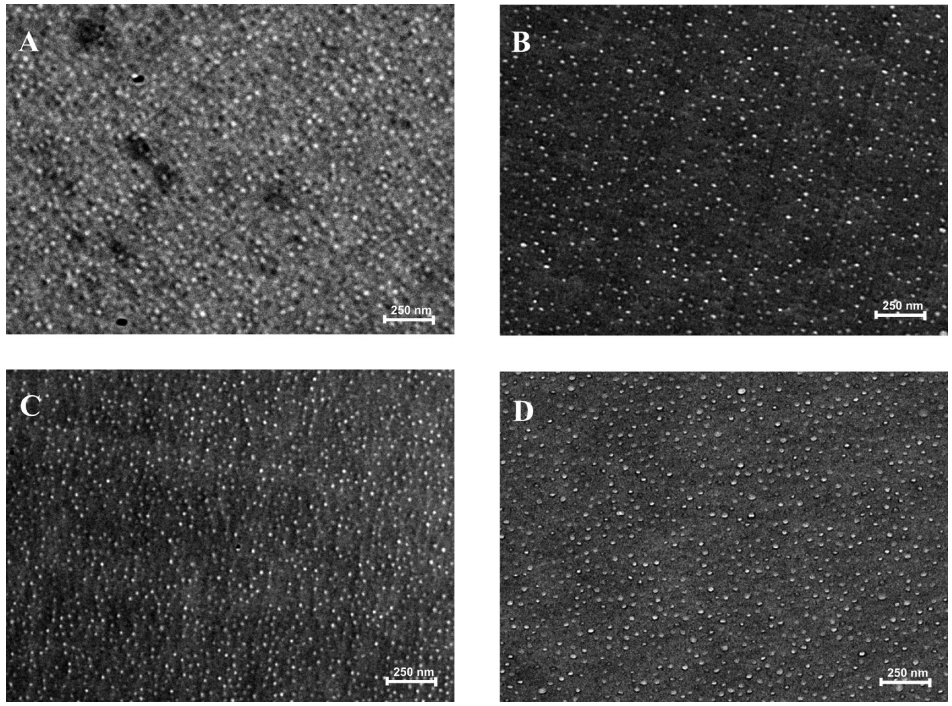

Figure 4. TEM micrographs of the thermosets containing (A) 10, (B) 20, (C) 30, and (D) 40 wt % of POSS[PCL-*b*-PTFEA]$_8$.

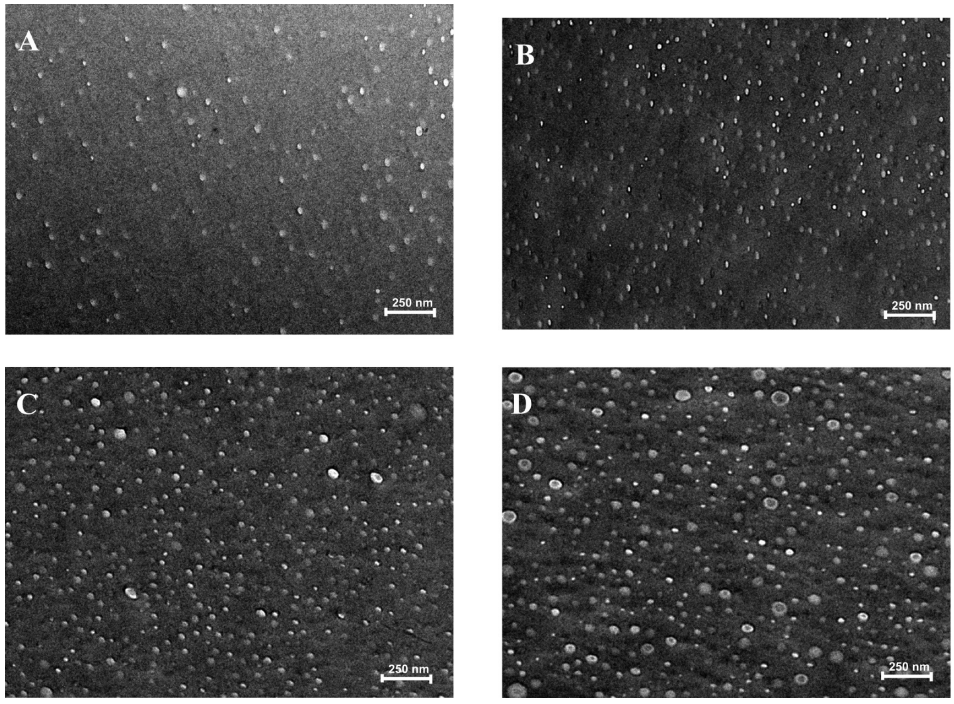

Figure 5. TEM micrographs of the thermosets containing (A) 10, (B) 20, (C) 30, and (D) 40 wt % of PCL-*b*-PTFEA diblock copolymer.

phenomenon and the intensity of the scattering peaks increased with increasing the content of the block copolymers. The results of SAXS indicate that the thermosets were indeed microphase-separated. In all the cases the broad and round scattering peaks were exhibited, which resulted from the form factor scattering of the spherical PTFEA microdomains dispersed in epoxy matrices as shown in Figures 4 and 5. Referring to the TEM results, we fitted the measured SAXS data with a model of hard sphere with polydispersity. The structure factor for hard spheres was fitted according to the Percus−Yevick closure relation.[55] The only interaction effect taken into account in this model is the excluded volume present in a dispersion of hard spheres. The polydispersity is taken into account by simply averaging the partial structure factor of the single components.[56] The intensity of scattering at a given scattering vector $[I(q)]$, depends on the square of the contrast difference $(\Delta\rho^2)$, the number of scattering particles (N), the shape and size of the scattering particle described by the form factor $[P(q)]$, and interdomain correlations accounted for by a structure factor $[S(q)]$:

dx.doi.org/10.1021/jp402084u | *J. Phys. Chem. B* 2013, 117, 8256−8268

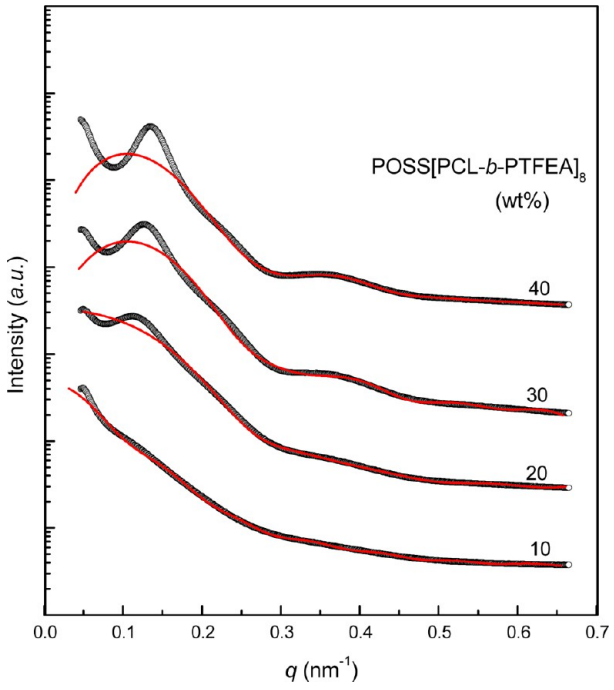

Figure 6. SAXS profiles of the epoxy thermosets containing star-like POSS[PCL-*b*-PTFEA]$_8$ block copolymers. The red lines represent the form factor scattering and were fitted according to Percus−Yevick closure relation.[55]

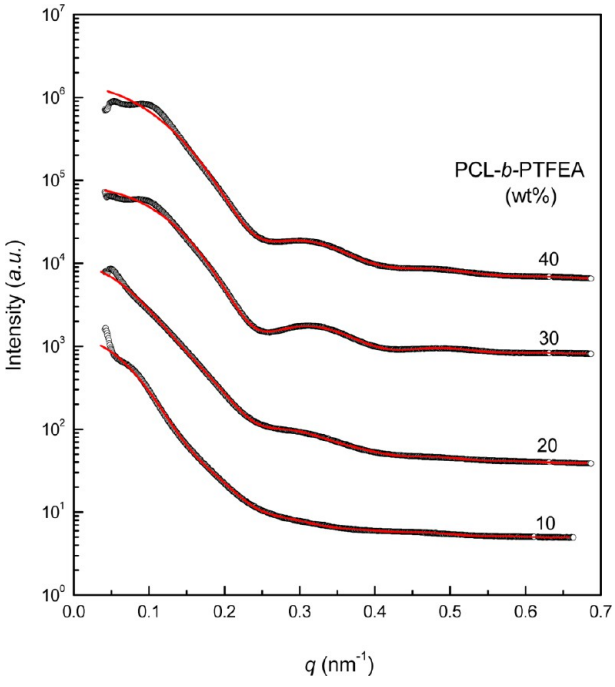

Figure 7. SAXS profiles of the epoxy thermosets containing PCL-*b*-PTFEA diblock copolymer. The red lines represent the form factor scattering and were fitted according to Percus−Yevick closure relation.[55]

$$I(q) = \Delta\rho^2 \times N \times P(q) \times S(q) \quad (1)$$

Assuming the PCL blocks (viz. corona) have essentially the same scattering density as the epoxy matrix (i.e., they are contrast-matched), the scattering arises almost from the contrast between the spherical PTFEA microdomains and the matrices composed of epoxy and PCL. The scattering of the spherical PTFEA microdomains is represented by the spherical form factor convoluted with a Gaussian distribution with a standard deviation (σ) to account for polydispersity in the radii of the spherical microdomains. The interparticle interaction was modeled as hard-sphere potentials between micelles with disordered (liquid-like) packing in a matrix as described by Ornstein and Zernike[57] and Percus and Yevick.[55] Also shown in Figures 6 and 7 are the form factor scattering [$P(q)$] and the fitted SAXS curves by considering both form factor and structural factor scattering [$S(q)$]. It is seen that the model can fit the measured data quite well, yielding the fitting parameters summarized in Table 2. The fitting results showed that for the thermosets containing POSS[PCL-*b*-PTFEA]$_8$ the radii of the spherical PTFEA microdomains were in the range 23−28 nm with a standard error of 0.12−0.30. For the thermosets containing PCL-*b*-PTFEA, the radii of the spherical PTFEA microdomains were measured to be in the range 27−34 nm with a standard error of ca. 0.30. It is worth noticing that with identical contents of the block copolymers [viz. POSS[PCL-*b*-PTFEA]$_8$ or PCL-*b*-PTFEA], the sizes of PTFEA microdomain for the thermosets containing POSS[PCL-*b*-PTFEA]$_8$ were significantly smaller than those containing PCL-*b*-PTFEA diblock copolymer. This result was in good agreement with the morphological observation by means of TEM shown in Figures 4 and 5.

The above nanostructured thermosets were subjected to dynamic mechanical thermal analysis (DMTA) to investigate the microphase-separated morphologies. Shown in Figures 8 and 9 are the DMTA curves of the nanostructured thermosets containing POSS[PCL-*b*-PTFEA]$_8$ and PCL-*b*-PTFEA diblock copolymer in the temperature range −80 to +200 °C. The control epoxy displayed a major transition at ca. 160 °C, which is attributable to the glass transition temperature (T_g) of this polymer. In addition, the cross-linked polymer possessed two β relaxations at −60 and +70 °C, respectively. The former is assignable to the hydroxyether structural units of amine-cross-linked epoxy thermoset whereas the latter to biphenyl structural units of bisphenol A.[58−60] For the nanostructured thermosets, there appeared the new peaks at ca. −10 °C besides the major peaks. The intensity of the new peaks increased with increasing the contents of the block copolymers. The new peaks are assignable to the glass transitions of PTFEA nanodomains. It is seen that the T_g's of PTFEA nanodomains remain invariant, irrespective of the content of the diblock copolymers. The appearance of two separated T_g's for the thermosets containing the block copolymers indicates that the thermosets were phase-separated, which is in good agreement with the results of TEM and SAXS.

It is seen that the T_g's of epoxy matrices gradually shifted to the lower temperatures with increasing content of the block copolymers. The decreased T_g's are ascribed to the plasticization of PCL blocks that possessed the T_g as low as −65 °C on epoxy matrices. Nonetheless, it is noted that the T_g's of the nanostructured thermosets containing POSS[PCL-*b*-PTFEA]$_8$ were significantly lower than those of the nanostructured thermosets containing PCL-*b*-PTFEA with identical contents of the block copolymers as shown in Figure 10. It is proposed that the following factors could affect the T_g's of epoxy matrices: (i) the free ends of PCL blocks in the matrices, which could introduce excess free volumes, (ii) the nanoreinforcement of POSS on polymer matrices[61−63] in the thermosets containing POSS[PCL-*b*-PTFEA]$_8$, and (iii) the

dx.doi.org/10.1021/jp402084u | J. Phys. Chem. B 2013, 117, 8256−8268

Table 2. Characterization of Microdomain Structures for the Mixtures Composed of DGEBA, MOCA, and POSS[PCL-*b*-PTFEA]$_8$ (and/or PCL-*b*-PTFEA)

		fitting parameters	
POSS[PCL-*b*-PTFEA]$_8$ (or PCL-*b*-PTFEA) (wt %)	microdomains of PTFEA	epoxy/POSS[PCL-*b*-PTFEA]$_8$	epoxy/PCL-*b*-PTFEA
10	sphere	R = 22.9 nm, σ = 0.30	R = 24.3 nm, σ = 0.12
20	sphere	R = 27.3 nm, σ = 0.24	R = 26.4 nm, σ = 0.30
30	sphere	R = 27.9 nm, σ = 0.28	R = 34.0 nm, σ = 0.16
40	sphere	R = 28.7 nm, σ = 0.31	R = 34.7 nm, σ = 0.22

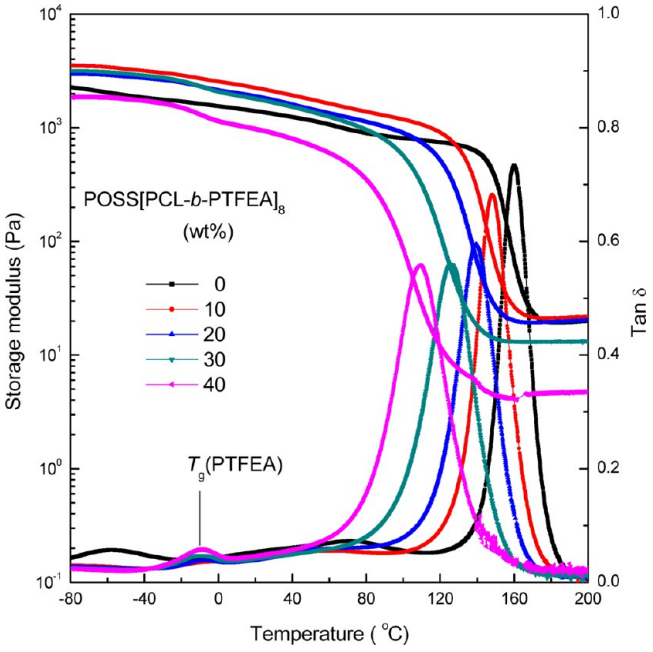

Figure 8. Dynamic mechanical spectra of the epoxy thermosets containing POSS[PCL-*b*-PTFEA]$_8$.

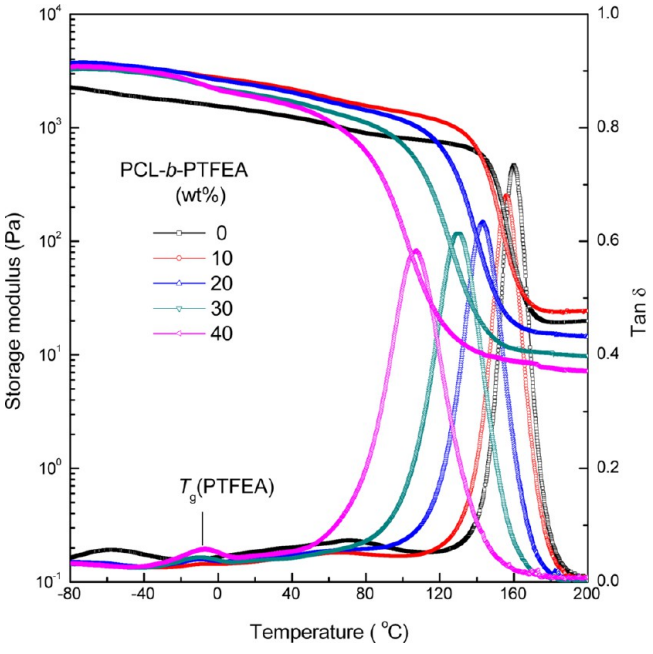

Figure 9. Dynamic mechanical spectra of the epoxy thermosets containing PCL-*b*-PTFEA diblock copolymer.

behavior of thermoset-philic block (viz. PCL) demixing out of epoxy matrix. In both nanostructured thermosetting systems,

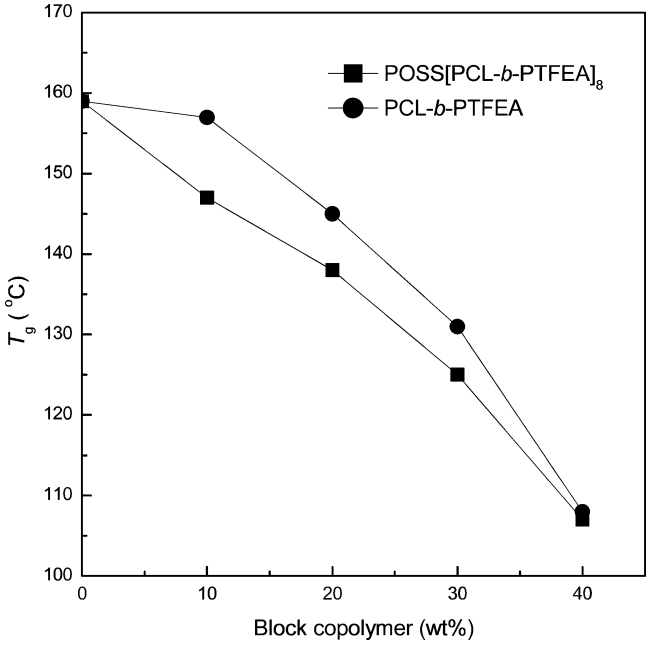

Figure 10. Plots of T_g's for epoxy matrices as functions of content of block copolymers.

the PCL blocks were miscible with the epoxy networks. In the thermosets containing PCL-*b*-PTFEA, however, each PCL block possessed one free end, which could introduce additional free volume and thus give rise to the additional decrease in T_g of the epoxy matrix. In marked contrast to the nanostructured thermosets containing PCL-*b*-PTFEA, no free ends of PCL blocks existed in the thermosets containing POSS[PCL-*b*-PTFEA]$_8$. In addition, there could be the nanoreinforcement of POSS in the thermosets containing POSS[PCL-*b*-PTFEA]$_8$, which would also cause the increased T_g's of epoxy matrices. If there were only the above effects, the nanostructured thermosets containing PCL-*b*-PTFEA would display the T_g's of epoxy matrices lower than those containing POSS[PCL-*b*-PTFEA]$_8$. Nonetheless, the results summarized in Figure 10 did not support this speculation. It has been realized that in the nanostructured thermosets containing the amphiphilic diblock copolymer[6] thermoset-philic blocks could be demixed from epoxy matrix to some extent with the occurrence of curing reaction. Such a demixing behavior has ever been interpreted as a transition from equilibrium morphology to a chemically pinned metastable state as the cross-linking reaction progresses through the gel point.[6] It is found that the demixing phenomenon is pronounced especially at low contents of amphiphilic block copolymers.[41,43,45,64] In the present cases, PCL blocks of the block copolymers behaved as the thermoset-philic block (i.e., PCL), which possessed the T_g of −65 °C much lower than that of control epoxy (viz. 159 °C).

dx.doi.org/10.1021/jp402084u | J. Phys. Chem. B 2013, 117, 8256−8268

Therefore, the behavior of PCL demixing out of epoxy matrix will result in the increase in T_g's of epoxy matrices. In terms of the values of T_g's measured by means of DMTA, it is proposed that there were more portions of PCL blocks demixed out of epoxy matrix in the nanostructured thermosets containing PCL-*b*-PTFEA than in the nanostructured thermosets containing POSS[PCL-*b*-PTFEA]$_8$. Furthermore, the behavior of PCL blocks demixing out of epoxy matrix is dominant among the above factors to affect the T_g's of epoxy matrices. It is proposed that the tendency that PCL blocks were demixed out of epoxy matrices could be significantly suppressed if the ends of PCL blocks were covalently bonded onto a nanosized silsesquioxane cage, i.e., while the POSS[PCL-*b*-PTFEA]$_8$ was used instead of PCL-*b*-PTFEA with identical contents of the block copolymers.

Interpretation of Nanostructure Formation. *Formation Mechanisms of Nanophases.* It is known that PCL is miscible with epoxy[64−66] whereas PTFEA is immiscible with epoxy after and before the curing reaction.[38] The difference in miscibility is reminiscent of incorporating the binary block copolymers composed of PCL and PTFEA into epoxy to access the nanostructured thermosets via the self-assembly approach. In this situation, the precursors of epoxy act as selective solvents of amphiphilic block copolymers and thus the self-assembly behavior of the block copolymers in their mixtures with the precursors of epoxy would be exhibited. The self-assembled nanostructures can be fixed by initiating the curing reactions of epoxy resin. Representatively shown in Figures 11 and 12 are

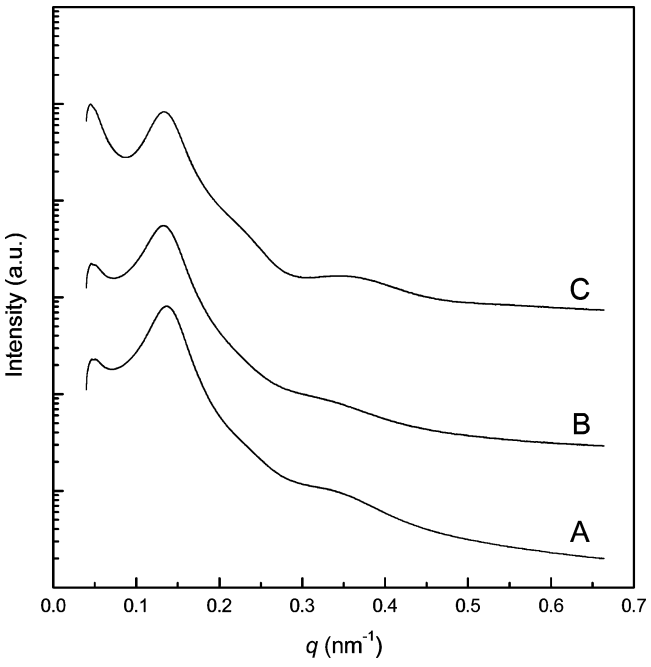

Figure 11. SAXS profiles of the mixture of the epoxy precursors with 40 wt % POSS[PCL-*b*-PTFEA]$_8$ at different temperatures: (A) at 80 °C, (B) at 150 °C; (C) after curing at 150 °C for 3 h plus 180 °C for 2 h.

the SAXS profiles of the mixtures of the epoxy precursors (viz. DGEBA + MOCA) with POSS[PCL-*b*-PTFEA]$_8$ (40 wt %) (and/or PCL-*b*-PTFEA diblock copolymer) after and before the curing reaction. For the mixture containing POSS[PCL-*b*-PTFEA]$_8$, the SAXS profile displayed the multiple scattering peaks at 80 °C, which was above the melting point of PCL block. While the mixture was rapidly heated up to the curing

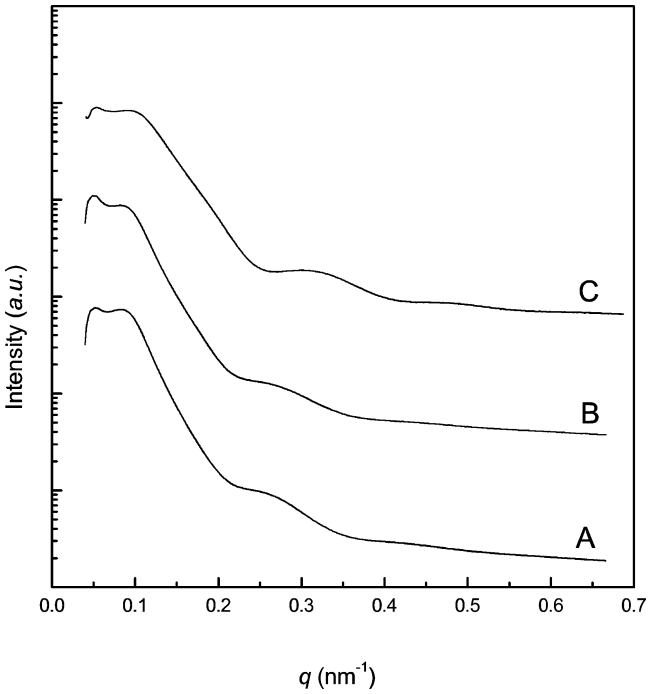

Figure 12. SAXS profiles of the mixture of the epoxy precursors with 40 wt % PCL-*b*-PTFEA diblock copolymer at different temperatures: (A) at 80 °C; (B) at 150 °C; (C) after curing at 150 °C for 3 h plus 180 °C for 2 h.

temperature (i.e., 150 °C), the position of multiple scattering peaks almost remained invariant but the scattering intensity was slightly decreased. The results of SAXS indicate that the block copolymer was capable of self-assembling in the epoxy precursors and the self-organized nanophases survived at the elevated temperature until the occurrence of the curing reaction. After cured at 150 °C for 3 h plus 180 °C for 2 h, the thermosets were obtained. It is seen that the cured thermoset possessed a scattering profile similar to that of the mixture of the epoxy precursors with the block copolymer but the intensity of scattering was significantly increased. The results of SAXS indicate that the nanostructured thermosets were indeed obtained via the approach of self-assembly followed by curing reaction. A similar situation was also found in the nanostructured thermosets containing PCL-*b*-PTFEA diblock copolymer.

Effect of Star-like Topology with POSS Core. The results of TEM and SAXS showed that there was a morphological difference between both nanostructured thermosetting systems, although both POSS[PCL-*b*-PTFEA]$_8$ and PCL-*b*-PTFEA block copolymers possessed identical compositions and lengths of blocks (viz. PCL and PTFEA). With identical contents of the block copolymers, the sizes of PTFEA microdomains in the nanostructured thermosets containing POSS[PCL-*b*-PTFEA]$_8$ were significantly lower than in those containing PCL-*b*-PTFEA$_8$. The morphological difference is attributable to the following factors: (i) the topologies of block copolymers and (ii) the phenomenon of PCL subchain demixing out of epoxy matrix. The different topologies of amphiphilic block copolymer resulted in the different conformations of thermoset-philic blocks (viz. PCL blocks) at the surface of the micelles. For the thermosets containing PCL-*b*-PTFEA diblock copolymer, the PCL subchains tended to take the conformation in which each PCL chain with one free end is

dx.doi.org/10.1021/jp402084u | J. Phys. Chem. B 2013, 117, 8256−8268

along the direction normal to the surface of PTFEA micelles. In marked contrast to the PTFEA micelle from the PCL-*b*-PTFEA diblock copolymer, the ends of every eight PCL subchains were "wrapped" onto a nanosized silsesquioxane cage (i.e., POSS) at the surface of the PTFEA micelles formed with POSS[PCL-*b*-PTFEA]$_8$ in epoxy (Scheme 2). All these PCL subchains at the surfaces of PTFEA microdomains were solubilized by the precursors of epoxy (viz. DGEBA + MOCA) and remained miscible with the cross-linked epoxy network. It is proposed that the sizes of PTFEA micelles are governed by the surface free energy of the micelles, which is dependent on the balance between epoxy precursors-phobicity and epoxy precursors-philicity. The fact that the sizes of PTFEA microdomains formed from POSS[PCL-*b*-PTFEA]$_8$ were significantly lower than those form PCL-*b*-PTFEA diblock copolymer suggests that with identical lengths of PCL chains, the surface free energy of the PTFEA micelles formed with POSS[PCL-*b*-PTFEA]$_8$ are lower than that of PTFEA micelles from PCL-*b*-PTFEA. It is an interesting question to investigate why such a PCL star with a POSS core can significantly depress the surface energy of micelles compared to linear PCL blocks. On the other hand, the morphological difference could be associated with the behavior of PCL demixing out of epoxy matrix with the occurrence of the curing reaction. The results of SAXS and DMTA showed that there were more portions of PCL blocks demixed out of epoxy matrix for the nanostructured thermosets containing PCL-*b*-PTFEA diblock copolymer than for the nanostructured thermosets containing POSS[PCL-*b*-PTFEA]$_8$. The demixed PCL subchains adhered to the surfaces of the PTFEA microdomains and the demixed PCL layer was formed. As a consequence, the sizes measured by means of TEM and SAXS were in reality the summation of the radii of PTFEA micelles and the thickness of the demixed PCL layer.

Scheme 2. Formation of Nanophases in the Thermosets Containing PCL-*b*-PTFEA and POSS[PCL-*b*-PTFEA]$_8$ Block Copolymers

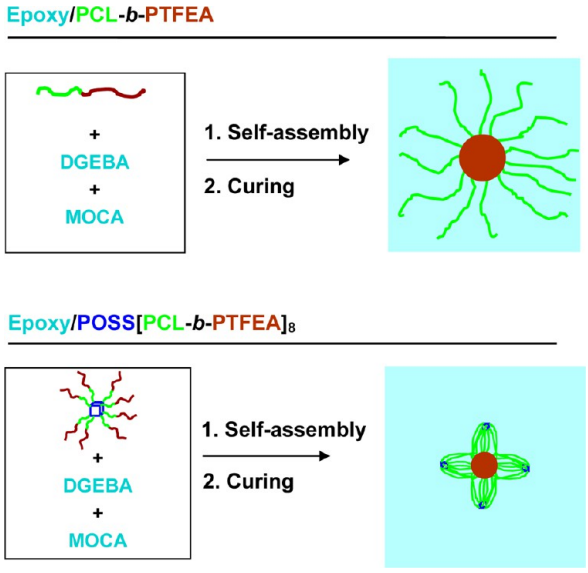

CONCLUSIONS

In this work, we synthesized two block copolymers with linear and star-like topologies. The block copolymers composed of poly(ε-caprolactone) (PCL) and poly(2,2,2-trifluoroethyl acrylate) (PTFEA) were successfully synthesized via the combination of ring-opening polymerization and reversible addition−fragmentation chain transfer/macromolecular design via the interchange of xanthate (RAFT/MADIX). Both block copolymers were controlled to have identical compositions of copolymerization and lengths of blocks. The star-like diblock copolymer contained with a polyhedral oligomeric silsesquioxane (POSS) core and eight PCL-*b*-PTFEA diblock copolymer arms. It is noted that the morphologies of the nanophases in the thermosets were quite dependent on the topological structures of the diblock copolymers. The spherical PTFEA nanophases were formed in these two thermosetting systems; however, the sizes of PTFEA microdomains formed from the star-like copolymer were significantly lower than those from the linear diblock copolymer. The dependence of the nanophases on the topologies of block copolymers is interpreted in terms of the conformation of the miscible subchain (viz. PCL) at the surface of PTFEA microdomains and the restriction of POSS cages on the demixing of the thermoset-philic block (viz. PCL).

AUTHOR INFORMATION

Corresponding Author

*Tel: 86-21-54743278. Fax: 86-21-54741297. E-mail: szheng@sjtu.edu.cn.

Notes

The authors declare no competing financial interest.

ACKNOWLEDGMENTS

The financial support from the Natural Science Foundation of China (No. 51133003 and 21274091) and National Basic Research Program of China (No. 2009CB930400) are gratefully acknowledged. The authors thank the Shanghai Synchrotron Radiation Facility for the support under the projects of Nos. 10sr0260 & 10sr0126.

REFERENCES

(1) Williams, R. J. J.; Rozenberg, B. A.; Pascault, J. P. Reaction-induced Phase Separation in Modified Thermosetting Polymers. *Adv. Polym. Sci.* **1997**, *128*, 95−156.

(2) Pascault, J. P.; Williams, R. J. J. In *Polymer Blends*; Paul, D. R., Bucknall, C. B., Eds.; Wiley: New York, 2000; pp 379−415.

(3) Ruiz-Pérez, L.; Royston, G. J.; Fairclough, J. A.; Ryan, A. J. Toughening by Nanostructure. *Polymer* **2008**, *49*, 4475−4488.

(4) Zheng, S. In *Epoxy Polymers: New Materials and Innovations*; Pascault, J. P., Williams, R. J. J., Eds.; Wiley-VCH: Weinheim, 2010; pp 79−108.

(5) Hillmyer, M. A.; Lipic, P. M.; Hajduk, D. A.; Almdal, K.; Bates, F. S. Self-Assembly and Polymerization of Epoxy-Resin Amphiphilic Block-Copolymer Nanocomposites. *J. Am. Chem. Soc.* **1997**, *119*, 2749−2750.

(6) Lipic, P. M.; Bates, F. S.; Hillmyer, M. A. Nanostructured Thermosets from Self-Assembled Amphiphilic Block Copolymer/Epoxy Resin Mixtures. *J. Am. Chem. Soc.* **1998**, *120*, 8963−8970.

(7) Meng, F.; Zheng, S.; Zhang, W.; Li, H.; Liang, Q. Nanostructured Thermosetting Blends of Epoxy Resin and Amphiphilic Poly(ε-caprolactone)-*block*-polybutadiene-*block*-poly(ε-caprolactone) Triblock Copolymer. *Macromolecules* **2006**, *39*, 711−719.

(8) Meng, F.; Zheng, S.; Li, H.; Liang, Q.; Liu, T. Formation of Ordered Nanostructures in Epoxy Thermosets: a Mechanism of Reaction-induced Microphase Separation. *Macromolecules* **2006**, *39*, 5072−5080.

(9) Dean, J. M.; Verghese, N. E.; Pham, H. Q.; Bates, F. S. Nanostructure Toughened Epoxy Resins. *Macromolecules* **2003**, *36*, 9267−9270.

(10) Liu, J.; Sue, H.-J.; Thompson, Z. J.; Bates, F. S.; Dettloff, M.; Jacob, G.; Verghese, N.; Pham, H. Nanocavitation in Self-Assembled Amphiphilic Block Copolymer-Modified Epoxy. *Macromolecules* **2008**, *41*, 7616−7624.
(11) Thompson, Z. J.; Hillmyer, M. A.; Liu, J.; Sue, H.-J.; Dettloff, M.; Bates, F. S. Block Copolymer Toughened Epoxy: Role of Cross-Link Density. *Macromolecules* **2009**, *42*, 2333−2337.
(12) Liu, J.; Sue, H.-J.; Thompson, Z. J.; Bates, F. S; Dettloff, M.; Jacob, G.; Verghese, N.; Pham, H. Strain Rate Effect on Toughening of Nano-Sized PEP−PEO Block Copolymer Modified Epoxy. *Acta Mater.* **2009**, *57*, 2691−2701.
(13) Valkama, S.; Nykaenen, A.; Kosonen, H.; Ramani, R.; Tuomisto, F.; Engelhardt, P.; Ten Brinke, G.; Ikkala, O.; Ruokolainen, J. Hierarchical Porosity in Self-Assembled Polymers: Post-Modification of Block Copolymer-Phenolic Resin Complexes by Pyrolysis Allows the Control of Micro-and Mesoporosity. *Adv. Funct. Mater.* **2007**, *17*, 183−190.
(14) Kosonen, H.; Ruokolainen, J.; Torkkeli, M.; Serimaa, R.; Nyholm, P.; Ikkala, O. Micro-and Macrophase Separation in Phenolic Resol Resin/PEO-PPO-PEO Block Copolymer Blends: Effect of Hydrogen-Bonded PEO Length. *Macromol. Chem. Phys.* **2002**, *203*, 388−392.
(15) Zhang, F.; Meng, Y.; Gu, D.; Yan, Y.; Chen, Z.; Tu, B.; Zhao, D. An Aqueous Cooperative Assembly Route To Synthesize Ordered Mesoporous Carbons with Controlled Structures and Morphology. *Chem. Mater.* **2006**, *18*, 5279−5288.
(16) Huang, Y.; Cai, H.; Yu, T.; Zhang, F.; Meng, Y.; Gu, D.; Wan, Y.; Sun, X.; Tu, B.; Zhao, D. Formation of Mesoporous Carbon With a Face-Centered-Cubic Fdm Structure and Bimodal Architectural Pores From the Reverse Amphiphilic Triblock Copolymer PPO-PEO-PPO. *Angew. Chem., Int. Ed.* **2007**, *46*, 1089−1092.
(17) Li, J.-G.; Lin, Y.-D.; Kuo, S.-W. From Microphase Separation to Self-Organized Mesoporous Phenolic Resin through Competitive Hydrogen Bonding with Double-Crystalline Diblock Copolymers of Poly(ethylene oxide-*b*-ε-caprolactone). *Macromolecules* **2011**, *44*, 9295−9309.
(18) Hu, D.; Xu, Z.; Zeng, K.; Zheng, S. From Self-Organized Novolac Resins to Ordered Nanoporous Carbons. *Macromolecules* **2010**, *43*, 2960−2969.
(19) Amendt, M. A.; Chen, L.; Hillmyer, M. A. Formation of Nanostructured Poly(dicyclopentadiene) Thermosets Using Reactive Block Polymers. *Macromolecules* **2010**, *43*, 3924−3934.
(20) Hu, D.; Zheng, S. Reaction-Induced Microphase Separation in Polybenzoxazine Thermosets Containing Poly(N-vinyl pyrrolidone)-*block*-polystyrene Diblock Copolymer. *Polymer* **2010**, *51*, 6346−6354.
(21) Mijovic, J.; Shen, M.; Sy, J. W.; Mondragon, I. Dynamics and Morphology in Nanostructured Thermoset Network/block Copolymer Blends during Network Formation. *Macromolecules* **2000**, *33*, 5235−5244.
(22) Grubbs, R. B.; Dean, J. M.; Broz, M. E.; Bates, F. S. Reactive Block Copolymers for Modification of Thermosetting Epoxy. *Macromolecules* **2000**, *33*, 9522−9534.
(23) Grubbs, R. B.; Dean, J. M.; Bates, F. S. Methacrylic Block Copolymers through Metal-mediated Living Free Radical Polymerization for Modification of Thermosetting Epoxy. *Macromolecules* **2001**, *34*, 8593−8595.
(24) Guo, Q.; Thomann, R.; Gronski, W. Phase Behavior, Crystallization, and Hierarchical Nanostructures in Self-Organized Thermoset Blends of Epoxy Resin and Amphiphilic Poly(ethylene oxide)-*block*-poly(propylene oxide)-*block*-poly(ethylene oxide) Triblock Copolymers. *Macromolecules* **2002**, *35*, 3133−3159.
(25) Ritzenthaler, S.; Court, F.; Girard-Reydet, E.; Leibler, L.; Pascault, J.-P. ABC Triblock Copolymers/epoxy-diamine Blends. 1. Keys to Achieve Nanostructured Thermosets. *Macromolecules* **2002**, *35*, 6245−6254.
(26) Ritzenthaler, S.; Court, F.; Girard-Reydet, E.; Leibler, L.; Pascault, J.-P. ABC Triblock Copolymers/epoxy-diamine Blends. 2. Parameters Controlling the Morphologies and Properties. *Macromolecules* **2003**, *36*, 118−126.
(27) Rebizant, V.; Abetz, V.; Tournihac, T.; Court, F.; Leibler, L. Reactive Tetrablock Copolymers Containing Glycidyl Methacrylate. Synthesis and Morphology Control in Epoxy−Amine Networks. *Macromolecules* **2003**, *36*, 9889−9896.
(28) Dean, J. M.; Verghese, N. E.; Pham, H. Q.; Bates, F. S. Nanostructure Toughened Epoxy Resins. *Macromolecules* **2003**, *36*, 9267−9270.
(29) Rebizant, V.; Venet, A. S.; Tournillhac, F.; Girard-Reydet, E.; Navarro, C.; Pascault, J.-P.; Leibler, L. Chemistry and Mechanical Properties of Epoxy-Based Thermosets Reinforced by Reactive and Nonreactive SBMX Block Copolymers. *Macromolecules* **2004**, *37*, 8017−8027.
(30) Dean, J. M.; Grubbs, R. B.; Saad, W.; Cook, R. F.; Bates, F. S. Mechanical Properties of Block Copolymer Vesicle and Micelle Modified Epoxies. *J. Polym. Sci., Part B: Polym. Phys.* **2003**, *41*, 2444−2456.
(31) Wu, J.; Thio, Y. S.; Bates, F. S. Structure and Properties of PBO-PEO Diblock Copolymer Modified Epoxy. *J. Polym. Sci., Part B: Polym. Phys.* **2005**, *43*, 1950−1965.
(32) Zucchi, I. A.; Galante, M. J.; Williams, R. J. J. Comparison of Morphologies and Mechanical Properties of Crosslinked Epoxies Modified by Polystyrene and Poly(methyl methacrylate) or by the Corresponding Block Copolymer Polystyrene-*b*-poly(methyl methacrylate). *Polymer* **2005**, *46*, 2603−2610.
(33) Thio, Y. S.; Wu, J.; Bates, F. S. Epoxy Toughening using Low Molecular Weight Poly(hexylene oxide)-poly(ethylene oxide) Diblock Copolymers. *Macromolecules* **2006**, *39*, 7187−7189.
(34) Serrano, E.; Tercjak, A.; Kortaberria, G.; Pomposo, J. A.; Mecerreyes, D.; Zafeiropoulos, N. E.; Stamm, M.; Mondragon, I. Nanostructured Thermosetting Systems by Modification with Epoxidized Styrene-butadiene Star Block Copolymers. Effect of Epoxidation Degree. *Macromolecules* **2006**, *39*, 2254−2261.
(35) Chen, J.-L.; Chang, F.-C. Phase Separation Process in Poly(ε-caprolactone)-Epoxy Blends. *Macromelecules* **1999**, *32*, 5348−5356.
(36) Maiez-Tribut, S.; Pascault, J.-P.; Soule, E. R.; Borrajo, J.; Williams, R. J. J. Nanostructured Epoxies Based on the Self-Assembly of Block Copolymers: A New Miscible Block That Can Be Tailored to Different Epoxy Formulations. *Macromolecules* **2007**, *40*, 1268−1273.
(37) Gong, W.; Zeng, K.; Wang, L.; Zheng, S. Poly(hydroxyether of bisphenol A)-*block*-polydimethylsiloxane Alternating Block Copolymer and Its Nanostructured Blends with Epoxy Resin. *Polymer* **2008**, *49*, 3318−3326.
(38) Yi, F.; Zheng, S.; Liu, T. Nanostructures and Surface Hydrophobicity of Self-Assembled Thermosets Involving Epoxy Resin and Poly(2,2,2-trifluoroethyl acrylate)-*block*-Poly(ethylene oxide) Amphiphilic Diblock Copolymer. *J. Phys. Chem. B* **2009**, *113*, 1857−1868.
(39) Meng, F.; Zheng, S.; Liu, T. Epoxy Resin Containing Poly(ethylene oxide)-*block*-poly(ε-caprolactone) Diblock Copolymer: Effect of Curing Agents on Nanostructures. *Polymer* **2006**, *47*, 7590−7600.
(40) Sinturel, C.; Vayer, M.; Erre, R.; Amenitsch, H. Nanostructured Polymers Obtained from Polyethylene-*block*-poly(ethylene oxide) Block Copolymer in Unsaturated Polyester. *Macromolecules* **2007**, *40*, 2532−2538.
(41) Ocando, C.; Serrano, E.; Tercjak, A.; Pena, C.; Kortaberria, G.; Calberg, C.; Grignard, B.; Jerome, R.; Carrasco, P. M.; Mecerreyes, D.; et al. Structure and Properties of a Semifluorinated Diblock Copolymer Modified Epoxy Blend. *Macromolecules* **2007**, *40*, 4068−4074.
(42) Xu, Z.; Zheng, S. Reaction-induced Microphase Separation in Epoxy Thermosets Containing Poly(ε-caprolactone)-*block*-poly(*n*-butyl acrylate) Diblock Copolymer. *Macromolecules* **2007**, *40*, 2548−2558.
(43) Meng, F.; Xu, Z.; Zheng, S. Microphase Separation in Thermosetting Blends of Epoxy Resin and Poly(ε-caprolactone)-*block*-Polystyrene Block Copolymers. *Macromolecules* **2008**, *41*, 1411−1420.

(44) Fan, W.; Zheng, S. Reaction-Induced Microphase Separation in Thermosetting Blends of Epoxy Resin with Poly(methyl methacrylate)-*block*-polystyrene Block Copolymers: Effect of Topologies of Block Copolymers on Morphological Structures. *Polymer* **2008**, *49*, 3157−3167.
(45) Fan, W.; Wang, L.; Zheng, S. Nanostructures in Thermosetting Blends of Epoxy Resin with Polydimethylsiloxane-*block*-poly(ε-caprolactone)-*block*-polystyrene ABC Triblock Copolymer. *Macromolecules* **2008**, *42*, 327−336.
(46) Ocando, C.; Tercjak, A.; Martín, M. D.; Ramos, J. A.; Campo, M.; Mondragon, I. Morphology Development in Thermosetting Mixtures through the Variation on Chemical Functionalization Degree of Poly(styrene-*b*-butadiene) Diblock Copolymer Modifiers. Thermomechanical Properties. *Macromolecules* **2009**, *42*, 6215−6224.
(47) Fan, W.; Wang, L.; Zheng, S. Double Reaction-induced Microphase Separation in Epoxy Resin Containing Polystyrene-*block*-poly(ε-caprolactone)-*block*-poly(*n*-butyl acrylate) ABC Triblock Copolymer. *Macromolecules* **2010**, *43*, 10600−10611.
(48) Serrano, E.; Larranaga, M.; Remiro, P. M.; Mondragon, I.; Carrasco, P. M.; Pomposo, J. A.; Mecerreyes, D. Synthesis and Characterization of Epoxidized Styrene-Butadiene Block Copolymers as Templates for Nanostructured Thermosets. *Macromol. Chem. & Phys.* **2004**, *205*, 987−996.
(49) Serrano, E.; Martin, M. D.; Tercjak, A.; Pomposo, J. A.; Mecerreyes, D.; Mondragon, I. Nanostructured Thermosetting Systems from Epoxidized Styrene Butadiene Block Copolymers. *Macromol. Rapid Commun.* **2005**, *26*, 982−985.
(50) Hameed, N.; Guo, Q.; Xu, Z.; Hanley, T. L.; Mai, Y.-W. Reactive Block Copolymer Modified Thermosets: Highly Ordered Nanostructures and Improved Properties. *Soft Matter* **2010**, *6*, 6119−6129.
(51) Wu, S.; Guo, Q.; Peng, S.; Hameed, N.; Kraska, M.; Stühn, B.; Mai, Y.-W. Toughening Epoxy Thermosets with Block Ionomer Complexes: A Nanostructure-Mechanical Property Correlation. *Macromolecules* **2012**, *45*, 3829−3840.
(52) Zhu, L.; Zhang, C.; Han, J.; Zheng, S.; Li, X. Formation of Nanophases in Epoxy Thermosets Containing an Organic-inorganic Macrocyclic Molecular Brush with Poly(ε-caprolactone)-*block*-polystyrene Side Chains. *Soft Matter* **2012**, *8*, 7062−7072.
(53) Fleet, R.; McLeary, J. B.; Grumel, V.; Weber, W. G.; Matahwa, H.; Sanderson, R. D. Preparation of New Multiarmed RAFT Agents for the Mediation of Vinyl Acetate Polymerization. *Macromol. Symp.* **2007**, *255*, 8−19.
(54) Jnkova, K.; Chen, X.; Kops, J.; Batsberg, W. *Macromolecules* **1998**, *31*, 538−541.
(55) Percus, J. K.; Yevick, G. Analysis of Classical Statistical Mechanics by Means of Collective Coordinates. *Phys. Rev.* **1958**, *110*, 1−13.
(56) Brunner-Popela, J.; Glatter, O. Small-Angle Scattering of Interacting Particles. I. Basic Principles of a Global Evaluation Technique. *J. Appl. Crystallogr.* **1997**, *30*, 431−442.
(57) Ornstein, L. S.; Zernike, F. Accidental Deviations of Density and Opalescence at the Critical Point in a Single Substance. *Proc. Akad. Sci. (Amsterdam)* **1914**, *17*, 793−806.
(58) Kline, D. E. Dynamic Mechanical Properties of Polymerized Epoxy Resins. *J. Polym. Sci.* **1960**, *47*, 237−249.
(59) Ochi, M.; Okasaki, M.; Shimbo, M. Mechanical Relaxation Mechanism of Epoxide Resins Cured with Aliphatic Diamines. *J. Polym. Sci., Part B: Polym Phys* **1982**, *20*, 689−699.
(60) Shibanov, Y. D.; Godovsky, Y. K. Interrelation of Phase and Relaxation Behavior in Polymer Blends and Block Copolymers with Crystallizable Components. *Relax. Polym.* **1989**, *80*, 110−118.
(61) Li, G.; Wang, L.; Ni, H.; Pittman, C. U. Polyhedral Oligomeric Silsesquioxane (POSS) Polymers and Copolymers: A Review. *J. Inorg. Organomet. Polym.* **2002**, *11*, 123−154.
(62) Laine, R. M.; Roll, M. F. Polyhedral Phenylsilsesquioxanes. *Macromolecules* **2011**, *44*, 1073−1109.
(63) Kuo, S.-W.; Chang, F.-C. POSS Related Polymer Nanocomposites. *Prog. Polym. Sci.* **2011**, *36*, 1649−1696.
(64) Yin, M.; Zheng, S. Ternary Thermosetting Blends of Epoxy Resin, Poly (ethylene oxide) and Poly (ε-caprolactone). *Macromol. Chem. Phys.* **2005**, *206*, 929−937.
(65) Ni, Y.; Zheng, S. Influence of Intramolecular Specific Interactions on Phase Behavior of Epoxy Resin and Poly(ε-caprolactone) Blends Cured with Aromatic Amines. *Polymer* **2005**, *46*, 5828−5839.
(66) Yi, F.; Yu, R.; Zheng, S.; Li, X. Nanostructured Thermosets from Epoxy and Poly(2,2,2-trifluoroethyl acrylate)-*block*-poly(glycidyl methacrylate) Diblock Copolymer: Demixing of Reactive Blocks and Thermomechanical Properties. *Polymer* **2011**, *52*, 5669−5680.